Thin-Film Magnetization Dynamics on the Surface of a Topological Insulator

Yaroslav Tserkovnyak[1] and Daniel Loss[2]

[1]Department of Physics and Astronomy, University of California, Los Angeles, California 90095, USA
[2]Department of Physics, University of Basel, Klingelbergstrasse 82, CH-4056 Basel, Switzerland

(Received 26 December 2011; published 30 April 2012)

We theoretically study the magnetization dynamics of a thin ferromagnetic film exchange coupled with a surface of a strong three-dimensional topological insulator. We focus on the role of electronic zero modes imprinted by domain walls (DWs) or other topological textures in the magnetic film. Thermodynamically reciprocal hydrodynamic equations of motion are derived for the DW responding to electronic spin torques, on the one hand, and fictitious electromotive forces in the electronic chiral mode fomented by the DW, on the other. An experimental realization illustrating this physics is proposed based on a ferromagnetic strip, which cuts the topological insulator surface into two gapless regions. In the presence of a ferromagnetic DW, a chiral mode transverse to the magnetic strip acts as a dissipative interconnect, which is itself a dynamic object that controls (and, inversely, responds to) the magnetization dynamics.

DOI: 10.1103/PhysRevLett.108.187201 PACS numbers: 75.70.−i, 72.15.Gd, 73.43.−f, 85.75.−d

Following theoretical predictions [1] and experimental realizations [2] of three-dimensional topological insulators (TIs), vigorous ongoing activities in this burgeoning field are aimed at introducing spontaneous symmetry breaking mechanisms into the system. This could be accomplished by bulk or surface doping to induce magnetism or superconductivity in the parent (essentially free-electron) TI, or by a heterostructure design wherein symmetry breaking is instilled at the TI surface by a quantum proximity effect. We are following the latter route, considering an insulating ferromagnetic layer (MI) capping the bulk TI, such that the TI surface states are exchange coupled to the collective magnetic moment of the MI. Previous theoretical investigations of a similar TI-MI heterostructure were concerned with current-induced spin torques experienced by a monodomain MI [3], Gilbert damping by a doped TI [4], electric charging of magnetic textures [5], and the rectification of charge pumping by a monodomain precession [6], all in case of a well-defined spatially uniform sign of the time-reversal symmetry breaking gap in the TI. The essential physical ingredient underlying the key ideas in these papers is the axion electrodynamics [7] associated with the TI [8], with a quantized magnetoelectric coupling that is odd under time reversal. In this Letter, we are interested in salient features associated with dynamic magnetic textures that imprint a spatially inhomogeneous gap onto the TI surface states, both in regard to its magnitude and sign. The latter, in particular, engenders electronic chiral modes at the magnetic domain boundaries [9], whose hydrodynamics become intricately coupled with magnetic precession.

According to the spin-charge helicity of the TI electronic states, the spin-transfer torques acting on the MI are locked with the self-consistent electronic charge currents in the TI. These currents, in turn, can respond to a combination of electromagnetic fields and fictitious forces induced by MI dynamics, having several distinct contributions: (i) two-dimensional (2D) surface currents related to the half-quantized anomalous Hall effect, whose sign depends on the orientation of the capping magnetic domain, (ii) persistent currents governed by the magnetization texture in the capping MI layer, and (iii) Fermi-level chiral currents along the domain walls (DWs) separating regions with an opposite Hall conductance. As an illustrative example, we will describe how the DW position and an internal coordinate that parametrizes its Bloch-to-Néel transformation are responding to a chiral TI current flowing along the DW. Considering the inverse charge current pumped by the DW dynamics, we highlight a peculiar structure of the Onsager reciprocity, which reverses the DW magnetization as well as the chirality of the associated electronic mode.

Our focus will be centered on a ferromagnetic DW separating regions with an out-of-plane magnetization direction deep into the respective domains (which is true for sufficiently thin films, e.g., CoFeB alloys [10]). See Fig. 1 for a schematic. Let us treat the DW as a stiff solitonic quasi-1D object, parallel to the y axis, whose translational motion and soft internal dynamics can be described by generalized coordinates [11]. To be specific, we start with the following generic free energy for an isolated magnetic film with magnetic spin texture $\mathbf{m}(\mathbf{r})$ ($|\mathbf{m}| \equiv 1$):

$$F_0[\mathbf{m}] = \frac{1}{2}\int d^2r\{A[(\partial_x\mathbf{m})^2 + (\partial_y\mathbf{m})^2] - Km_z^2\}, \quad (1)$$

where A is the exchange stiffness parameter and $K > 0$ is the out-of-plane anisotropy constant. A one-dimensional DW running along the y axis and separating magnetic domains with $m_z = \pm 1$ at $x \to \pm\infty$, which minimizes free-energy (1), is then given in polar angles by

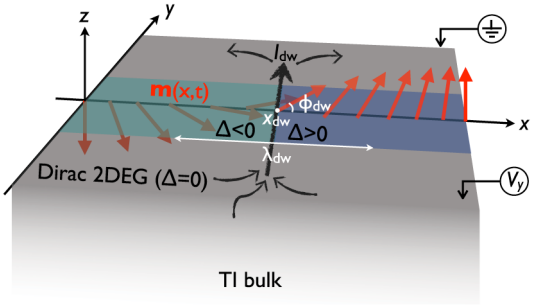

FIG. 1 (color online). Schematic of a DW in a ferromagnetic strip with an out-of-plane easy (z) axis anisotropy, deposited on the surface of a TI. The DW (of width $\lambda_{\rm dw}$) is parametrized, according to Eq. (2), by two *soft* dynamic coordinates: its position $x_{\rm dw}(t)$ and azimuthal angle $\phi_{\rm dw}(t)$. At the DW position, $x_{\rm dw}$, the magnetization $\mathbf{m}$ lies fully in the xy plane (forming angle $\phi_{\rm dw}$ with the x axis). A chiral electron mode (of width $\xi \ll \lambda_{\rm dw}$) formed in the TI under the DW carries transport current $I_{\rm dw}$ at its *exit* point, which is governed by the voltage V_y applied to the TI surface at its *entrance* and the fictitious electromotive force generated by the DW dynamics along its length. An Onsager-reciprocal spin torque affects DW dynamics in the presence of $I_{\rm dw}$.

$$\theta(\mathbf{r}) = 2\tan^{-1} e^{-(x-x_{\rm dw})/\lambda_{\rm dw}}, \qquad \phi(\mathbf{r}) = \phi_{\rm dw}, \tag{2}$$

which parametrize the position $\mathbf{r} \equiv (x, y)$-dependent magnetization direction $\mathbf{m} = (\sin\theta\cos\phi, \sin\theta\sin\phi, \cos\theta)$. $\lambda_{\rm dw} = \sqrt{A/K}$ is the DW width. The DW energy is degenerate with respect to the position $x_{\rm dw}$ and the azimuthal angle $\phi_{\rm dw}$. In particular, if $\phi = 0$ or π we have a Néel wall, and if $\phi = \pm\pi/2$ we have a Bloch wall. In practice, however, the degeneracy with respect to $x_{\rm dw}$ is lifted by spatial pinning fields, while the degeneracy with respect to $\phi_{\rm dw}$ by a homogeneous applied field or spin anisotropy (induced, e.g., by spin-orbit interactions) in the xy plane, which we will take account of below. For sufficiently gentle perturbations of this kind, the zero modes associated with $x_{\rm dw}(t)$ and $\phi_{\rm dw}(t)$ are thus converted into soft collective excitations, which are at the core of our analysis.

We now set out to develop a self-consistent hydrodynamic theory for a DW bound with a gapless chiral mode, which interacts with regions of incompressible TI Hall fluids flanking it on the sides. The introductory material on magnetoelectric properties of the TI, its exchange coupling to the MI, and the emergence of a chiral mode bound to a DW is relegated to the Supplemental Material [12]. From the electronic-structure point of view, the chiral mode patches two quantum Hall regions whose Chern number [13] changes by unity, between the values of $\pm 1/2$ imprinted by the magnetic domains. The underlying magnetoelectric effect is fundamentally distinct from the one discussed in Ref. [5], as the DW here coexists with the parity-anomaly point $m_z = 0$.

A complete picture of our coupled magnetohydrodynamic system requires us to consider also the spin-transfer torque that is reciprocal to the DW-driven electromotive forces [14]. Such torque acting on the magnetization is given, due to the MI-TI exchange (see [12] for details),

$$H' = J(m_x\hat{\sigma}_x + m_y\hat{\sigma}_y) + J_\perp m_z\hat{\sigma}_z, \tag{3}$$

by (within the Landau-Lifshitz phenomenology [15])

$$S\partial_t\mathbf{m}|_\tau = \langle\delta_{\mathbf{m}}H'\rangle \times \mathbf{m} = (J\boldsymbol{\sigma}_{xy} + J_\perp\sigma_z\mathbf{z}) \times \mathbf{m}. \tag{4}$$

Here, $\boldsymbol{\sigma} \equiv (\sigma_x, \sigma_y, \sigma_z) \equiv (\boldsymbol{\sigma}_{xy}, \sigma_z)$ is the TI surface spin density (defined by $\boldsymbol{\sigma} = \langle\hat{\boldsymbol{\sigma}}\rangle$, in terms of Pauli matrices $\hat{\boldsymbol{\sigma}}$) and S is the saturation spin density of the ferromagnet. It follows from the Dirac Hamiltonian, $H_0 = v(\mathbf{p} - e\mathbf{A}) \cdot \mathbf{z} \times \hat{\boldsymbol{\sigma}} + e\varphi$, furthermore, that the in-plane spin density $\boldsymbol{\sigma}_{xy}$ is essentially equivalent to the charge current density, since

$$\mathbf{j} = -\langle\delta_{\mathbf{A}}H\rangle = ev\mathbf{z} \times \boldsymbol{\sigma} \Rightarrow \boldsymbol{\sigma}_{xy} = (ev)^{-1}\mathbf{j} \times \mathbf{z}. \tag{5}$$

Equation (5) is an exact identity between the total (i.e., equilibrium plus nonequilibrium) current density and the in-plane spin density of the TI electrons, which is unspoiled by electron-electron interactions and ferromagnetic proximity. In particular, the chiral states, which propagate in the y direction and have spin quantized along the x axis, carry a 2D equilibrium current density that is estimated as (see [12] for details)

$$\mathbf{j} \sim (ev/\xi)(\delta_{\rm dw}/2\pi\hbar v)\mathbf{z} \times \mathbf{x} \sim (e/2\pi\hbar)J_\perp\partial_x m_z\mathbf{y}, \tag{6}$$

where we put $\delta_{\rm dw} \sim \xi J_\perp\partial_x m_z$ for the chiral-mode bandwidth in terms of the characteristic (spatial) chiral-mode width ξ. From a purely phenomenological perspective, on the other hand, an equilibrium charge current associated with a smooth static texture is given, to the first order in general magnetic inhomogeneities, by

$$\mathbf{j} = \eta J_\perp\mathbf{z} \times \boldsymbol{\nabla}m_z, \tag{7}$$

which should be valid both near and away from the DW, as long as the current is analytic in the magnetic texture $\mathbf{m}(\mathbf{r})$. This current is time-reversal odd, mirror symmetric (in the xy plane), and divergenceless. We, furthermore, remark that it does not contradict the well-known result for the electromagnetic response of Dirac electrons [16], which is exact only for a strictly homogeneous system. The phenomenological coefficient η can, in general, be a function of $(J_\perp m_z)^2$, which we take to be constant in the limit of the weak exchange $J_\perp$. Comparing Eqs. (6) and (7), we conclude that $\eta \sim e/2\pi\hbar$ in our model, which is suggestive of a universal result (as long as $\xi \ll \lambda_{\rm dw}$).

In the presence of an equilibrium texture-induced current, the spin torque is given by

$$S\partial_t\mathbf{m}|_\tau = \delta_{\mathbf{m}}F_\tau \times \mathbf{m}, \tag{8}$$

in terms of the TI free-energy functional $F_\tau[\mathbf{m}]$ engendered by the MI-TI exchange. According to Eq. (7), this free-energy F_τ can be explicitly found by integrating

$$\delta_{\mathbf{m}_{xy}} F_\tau = J\boldsymbol{\sigma}_{xy} = (J/ev)\mathbf{j}\times\mathbf{z} = (\eta JJ_\perp/ev)\boldsymbol{\nabla} m_z \quad (9)$$

over $\mathbf{m}_{xy}$, at a fixed m_z [17]:

$$F_\tau = (\eta JJ_\perp/ev)\int d^2r\mathbf{m}\cdot\boldsymbol{\nabla} m_z + F'_\tau[m_z], \quad (10)$$

where F'_τ is a functional of m_z only [which therefore must derive entirely from the $J_\perp$ exchange in Eq. (3)]. To the leading order in the MI-TI exchange coupling $J_\perp$, F'_τ contributes merely to the out-of-plane anisotropy K in Eq. (1), which can be absorbed by a redefinition $K \to K + \mathcal{O}(J_\perp^2) \equiv K_*$. Higher-order terms in F'_τ, including those that depend on spatial inhomogeneities in m_z, would appear only at order $J_\perp^4$ (while cubic terms are prohibited by the time-reversal invariance). The leading-order MI-TI exchange coupling thus produces an anisotropy $\propto JJ_\perp$, which enhances the tendency to form magnetic textures (such as Skyrmion lattices), and a texture-independent (easy-axis) out-of-plane anisotropy $\propto J_\perp^2$, corresponding to the first and second terms in Eq. (10), respectively.

In addition to the equilibrium current density (7), there are also surface currents driven by the real and fictitious electromagnetic fields and the current carried by the gapless chiral mode. The latter may result in dissipation if connected to reservoirs (such as ungapped TI regions). All these currents contribute to the torque (4). [If $I_{\rm dw}$ is the 1D chiral *current*, the corresponding 2D *current density* in the y direction is $j_{\rm dw} \approx I_{\rm dw}\delta(x - x_{\rm dw})$, which is localized on the scale of the chiral-mode width ξ.] In particular, as discussed in the Supplemental Material [12], the torques arising from the effective electric-field-induced currents correspond to the Chern-Simons action associated with the effective 3-potential $\mathcal{A}_\mu \equiv A_\mu + a_\mu$ [with $A_\mu = (\varphi, -\mathbf{A})$ denoting the physical and $a_\mu = (0, -\mathbf{a})$, where $\mathbf{a} = (J/ev)\mathbf{m}\times\mathbf{z}$, the exchange-induced contributions].

Henceforth, focusing on the configuration sketched in Fig. 1, a finite-length DW cuts across a ferromagnetic strip connecting semi-infinite gapless 2D reservoirs flanking its sides. In this case, the reservoirs provide an equilibration and dissipation mechanism for the dc transport. In particular, at low frequencies, the chiral current is given by the Landauer-Büttiker formula [18]

$$I_{\rm dw} = g_Q\int_{\rm DW} dy\mathcal{E}_y \equiv g_Q\mathcal{V}_y \quad (11)$$

for the current in the y direction in response to the total effective field $\mathcal{E}_y$ applied along the DW length (the magnetic strip width). $\mathcal{V}_y = V_y + v_y$ is the corresponding effective voltage (V_y applied and v_y induced by magnetic dynamics) and $g_Q \equiv e^2/h$ is the conductance quantum. The current $I_{\rm dw}$ in Eq. (11) is defined at the *exit* point of the chiral mode and, concerning the applied voltage V_y, only the effective electric field along the DW *wire* and the chemical potential applied to the *entrance* point of the chiral mode need to be included. The chemical potential at the exit point of the chiral mode, on the other hand, has no effect on the current (at both the exit and the entrance) in the corresponding DW. We emphasize that the current *entering* the chiral mode can generally be distinct from $I_{\rm dw}$. In particular, the dynamically induced voltage v_y, as well as the voltage due to an electric field applied along the DW, does not affect the entrance current, which is fully governed by the chemical potential applied at the respective lead. In this case, any imbalance between the currents at the ends of the DW is absorbed by the gapped 2D regions flanking the chiral mode [in accordance with the effective magnetic field $\mathcal{B}_z = B_z + b_z$ [16], where $b_z \equiv \mathbf{z}\cdot\boldsymbol{\nabla}\times\mathbf{a} = -(J/ev)\boldsymbol{\nabla}\cdot\mathbf{m}$ is the texture-induced field], which we schematically sketch in the bottom panel of Fig. 2. Since the currents entering and exiting each individual DW thus depend very sensitively on the electrostatic considerations concerning the breakdown of the effective electrochemical potentials into the electric and chemical counterparts, we will focus on the noninteracting (i.e., well-screened) electrons driven by a combination of a

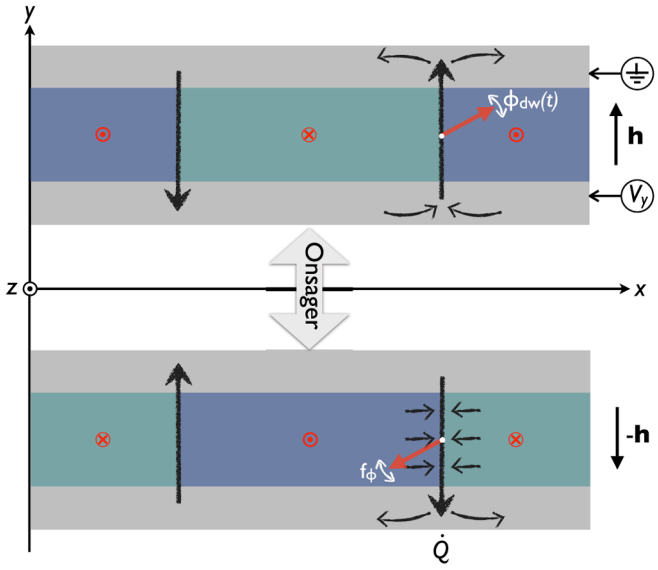

FIG. 2 (color online). The Onsager reciprocity relates voltage-induced DW dynamics (via spin torques) in the top panel [Eq. (14)] to the magnetization-dynamics-generated current (via fictitious electromotive force) in the bottom panel [Eq. (16)]. Note that the DWs in the bottom panel are mapped back onto their time-reversed parents in the top panel by a π rotation in the xy plane. This means that $\dot{Q}$ pumped by $\dot{\phi}_{\rm dw}$ for the right chiral mode is the same in both panels. The left DW is treated as pinned (and thus magnetically inert) in our treatment. However, when the electron-electron interactions are taken into account, electrostatic charge imbalance produced by fictitious forces near one DW could induce currents also along the other DW, making such a double-DW system generally coupled.

chemical-potential bias at the leads and magnetization dynamics along the DW.

We are now fully equipped to derive the equations of motion for the collective soft DW coordinates $x_{\rm dw}(t)$ and $\phi_{\rm dw}(t)$ that parametrize the DW position and internal structure according to Eq. (2). In the presence of the (equilibrium and nonequilibrium) current-induced spin torques [corresponding to Eqs. (10) and (11), respectively] as well as a uniform magnetic field h applied in the y direction, the full Landau-Lifshitz-Gilbert equation [15] for the magnetization dynamics becomes

$$S(1+\alpha\mathbf{m}\times)\partial_t\mathbf{m} = \mathbf{m}\times\mathbf{H}_*, \tag{12}$$

where α is the dimensionless Gilbert damping constant and the total effective field [including the usual Larmor piece $\mathbf{H}_{\rm eff} \equiv -\delta_{\mathbf{m}}F_0$ and the spin torques] is given by

$$\mathbf{H}_* = A\partial_x^2\mathbf{m} + K_* m_z\mathbf{z} + h\mathbf{y} + \eta_*(\mathbf{z}\partial_x m_x - \mathbf{x}\partial_x m_z) - j_*\mathbf{x}\delta(x-x_{\rm dw}). \tag{13}$$

Here, $\eta_* \equiv \eta J J_\perp/e\upsilon$ (with $\eta \sim e/2\pi\hbar$), according to Eq. (10), and $j_* = (J/e\upsilon)\bar{I}_{\rm dw}$, according to Eq. (5). $\bar{I}_{\rm dw}$ is the *average* transport current flowing under the DW along the y axis [19]. η_* and j_* thus parametrize the equilibrium and nonequilibrium spin torques, respectively.

The equations of motion for the generalized coordinates $\{q_i\} \equiv \{x_{\rm dw}, \phi_{\rm dw}\}$ are derived from Eqs. (12) and (13) by integrating Eq. (12), $\int d^2r\,\partial_{q_i}\mathbf{m}\cdot\{\mathbf{m}\times[S(1+\alpha\mathbf{m}\times)\partial_t\mathbf{m} = \mathbf{m}\times\mathbf{H}_*]\}$ [11], upon substitution of ansatz (2). The key underlying physical assumption in this procedure is that the internal DW structure is dominated by the A and K_* terms in Eq. (13), such that it has a fixed width $\lambda_{\rm dw} \approx \sqrt{A/K_*}$, while the dynamics of slow variables q_i are governed by the other terms in Eq. (13). Carrying out this program, we get (after a somewhat tedious but straightforward calculation) the following simple equations:

$$\dot{x}_{\rm dw} = -\frac{f_\phi + j_*\sin\phi_{\rm dw}}{(4+\alpha^2)S}, \qquad \dot{\phi}_{\rm dw} = -\frac{\alpha}{2\lambda_{\rm dw}}\dot{x}_{\rm dw}. \tag{14}$$

Here,

$$f_\phi \equiv -\frac{1}{L}\partial_{\phi_{\rm dw}}F = \frac{\eta_*\pi}{2}\sin\phi_{\rm dw} + h\lambda_{\rm dw}\pi\cos\phi_{\rm dw} \tag{15}$$

is the generalized force (per unit of DW length L) thermodynamically conjugate to the angle $\phi_{\rm dw}$. Since the domain wall is not pinned in the x direction, the force $-\partial_{x_{\rm dw}}F$ conjugate to $x_{\rm dw}$ vanishes in our model. The energy dissipation $P \equiv -(\partial_{\phi_{\rm dw}}F)\dot{\phi}_{\rm dw} - (\partial_{x_{\rm dw}}F)\dot{x}_{\rm dw}$ associated with magnetic dynamics (in the absence of transport current j_*) is thus guaranteed to be positive in an out-of-equilibrium situation when $\alpha > 0$. The spin-torque-driven DW dynamics in Eq. (14) reminds us of a dc Josephson effect ($\dot{Q} \propto \sin\varphi$). It is, in particular, noteworthy that the equilibrium and nonequilibrium spin torques add up, such that the latter can be formally absorbed into a redefinition of η_*: $\eta_* \to \eta_* + 2j_*/\pi$. In the absence of the applied field, $h = 0$, the dynamics would thus settle down at $\phi_{\rm dw} = 0$ or π (a Néel wall), for $\eta_* \lessgtr 0$ (corresponding to the ordinary or π Josephson junction, respectively). In the absence of spin torques but a finite field h along the y axis, the dynamics (that are overdamped as $\dot{\phi}_{\rm dw} \propto f_\phi$) would flow toward $\phi_{\rm dw} = \pm\pi/2$ (a Bloch wall), for $h \gtrless 0$, which corresponds to the lowest magnetostatic energy.

Supplementing Eqs. (14) with the Onsager reciprocity principle [20], dictates how the DW dynamics induce transport current along the chiral mode. (See Fig. 2.) To infer this, consider a voltage V_y-induced current: $j_* = (g_Q J/e\upsilon)V_y$. From Eqs. (14) and (15), which describe how this voltage induces dynamics ($\dot{x}_{\rm dw}$, $\dot{\phi}_{\rm dw}$), we recover their Onsager (time-reversed) counterpart in the charge sector:

$$\dot{Q} = \frac{g_Q J}{e\upsilon}\frac{\alpha\sin\phi_{\rm dw}}{2\lambda_{\rm dw}(4+\alpha^2)S}\partial_{\phi_{\rm dw}}F \to -\frac{g_Q J}{e\upsilon}L\dot{\phi}_{\rm dw}\sin\phi_{\rm dw} = \frac{g_Q J}{e\upsilon}L\partial_t m_x(x_{\rm dw}), \tag{16}$$

where on the second line we dropped the term that is diagonal in the charge sector and thus outside of the reciprocal reasoning [21]. In the final equality of Eq. (16), we recognize exactly the Landauer-Büttiker formula (11) for the magnetization-dynamics-driven charge current. It is crucial to notice that the DW chirality flips under time reversal, as illustrated in Fig. 2. The charge Q in Eq. (16) pumped by the DW dynamics in the top panel of Fig. 2 thus enters the reservoir that is opposite to the one where the voltage V_y is applied, as must be since $\dot{\phi}_{\rm dw}$ certainly induces the current only downstream of the chiral mode. This proves internal consistency of our theory.

In summary, we developed a self-consistent hydrodynamic description of a magnetic DW bound with its parity-anomaly chiral electron mode. DW dynamics parametrized by slow variables $x_{\rm dw}$ and $\phi_{\rm dw}$ share similarities with ac/dc Josephson relations for charge and phase, respectively. In particular, the DW switches between two types of Néel walls (corresponding to 0 and π junctions) depending on the sign of the spin torque, and two types of Bloch walls depending on the sign of the applied field. Reciprocally, the chiral transport is pumped by the DW dynamics, in accord with fictitious gauge fields along the DW length. This coupled system provides a ballistic electron interconnect, which can be imprinted onto TI surfaces and dynamically controlled by magnetic fields, opening rich possibilities for ''magnetic lithography'' of electronic nanostructures on TI surfaces.

This work was supported by the Alfred P. Sloan Foundation, DARPA, the NSF under Grant No. DMR-0840965 (Y. T.), and by the Swiss NSF (D. L.). Discussions with M. Z. Hasan are gratefully acknowledged. Y. T. is grateful for hospitality at the

University of Basel, where most of this work has been carried out.

[1] O. A. Pankratov, S. V. Pakhomov, and B. A. Volkov, Solid State Commun. **61**, 93 (1987); L. Fu, C. L. Kane, and E. J. Mele, Phys. Rev. Lett. **98**, 106803 (2007); J. E. Moore and L. Balents, Phys. Rev. B **75**, 121306 (2007); R. Roy, *ibid.* **79**, 195322 (2009).

[2] D. Hsieh, D. Qian, L. Wray, Y. Xia, Y. S. Hor, R. J. Cava, and M. Z. Hasan, Nature (London) **452**, 970 (2008); Y. Xia, D. Qian, D. Hsieh, L. Wray, A. Pal, H. Lin, A. Bansil, D. Grauer, Y. S. Hor, R. J. Cava, and M. Z. Hasan, Nature Phys. **5**, 398 (2009).

[3] I. Garate and M. Franz, Phys. Rev. Lett. **104**, 146802 (2010).

[4] T. Yokoyama, J. Zang, and N. Nagaosa, Phys. Rev. B **81**, 241410 (2010).

[5] K. Nomura and N. Nagaosa, Phys. Rev. B **82**, 161401 (2010).

[6] H. T. Ueda, A. Takeuchi, G. Tatara, and T. Yokoyama, Phys. Rev. B **85**, 115110 (2012).

[7] F. Wilczek, Phys. Rev. Lett. **58**, 1799 (1987).

[8] X.-L. Qi, T. L. Hughes, and S.-C. Zhang, Phys. Rev. B **78**, 195424 (2008).

[9] M. Z. Hasan and C. L. Kane, Rev. Mod. Phys. **82**, 3045 (2010).

[10] S. Ikeda, K. Miura, H. Yamamoto, K. Mizunuma, H. D. Gan, M. Endo, S. Kanai, J. Hayakawa, F. Matsukura, and H. Ohno, Nature Mater. **9**, 721 (2010).

[11] A. A. Thiele, Phys. Rev. Lett. **30**, 230 (1973); O. A. Tretiakov, D. Clarke, G.-W. Chern, Y. B. Bazaliy, and O. Tchernyshyov, *ibid.* **100**, 127204 (2008).

[12] See Supplemental Material at http://link.aps.org/supplemental/10.1103/PhysRevLett.108.187201 for magnetoelectric properties of topological insulator surfaces.

[13] D. J. Thouless, M. Kohmoto, M. P. Nightingale, and M. den Nijs, Phys. Rev. Lett. **49**, 405 (1982).

[14] Y. Tserkovnyak and C. H. Wong, Phys. Rev. B **79**, 014402 (2009).

[15] E. M. Lifshitz and L. P. Pitaevskii, *Statistical Physics, Part 2*, Course of Theoretical Physics, Vol. 9 (Pergamon, Oxford, 1980), 3rd ed; T. L. Gilbert, IEEE Trans. Magn. **40**, 3443 (2004).

[16] A. N. Redlich, Phys. Rev. Lett. **52**, 18 (1984); R. Jackiw, Phys. Rev. D **29**, 2375 (1984).

[17] The technical caveat that $\mathbf{m}$ is a unit vector is of no consequence here, as we are calculating the free energy of the TI electrons associated with the perturbation H', Eq. (3), which, in turn, can be thought of as parametrized by three independent variables (m_x, m_y, m_z).

[18] Y. V. Nazarov and Y. M. Blanter, *Quantum Transport* (Cambridge University Press, Cambridge, 2009).

[19] In our setup, $\bar{I}_{\rm dw} = g_Q \bar{\mathcal{V}}_y$, where $\bar{\mathcal{V}}_y = V_y + v_y/2$, as the dynamics-induced electromotive force v_y induces current strictly downstream along the chiral mode (and thus the *average* current $\bar{I}_{\rm dw}$ is half of the corresponding *exit* current $I_{\rm dw}$).

[20] L. D. Landau and E. M. Lifshitz, *Statistical Physics, Part 1*, Course of Theoretical Physics, Vol. 5 (Pergamon, Oxford, 1980), 3rd ed.

[21] Such terms correspond to $\mathcal{O}(J^2)$ corrections to various diagonal coefficients of the coupled system, which are outside of the scope and interest of this work.